U-Pb SHRIMP ZIRCON AGES FOR THE RIO APA CRATONIC FRAGMENT IN MATO GROSSO DO SUL (BRAZIL) AND NORTHERN PARAGUAY: TECTONIC IMPLICATIONS

Cordani, U.G., Tassinari, C.C.G., Teixeira, W. and Coutinho, J.M.V.

Institute of Geosciences, University of São Paulo – Rua do Lago 562 – 05508-080 São Paulo, Brazil. E-mail: ucordani@usp.br

Keywords: geochronology, South America, zircon, tectonic evolution.

ABSTRACT

In the northern part of the Rio Apa cratonic fragment, granitoid gneisses predominate, intruded by the granitic bodies of the Alumiador Intrusive Suite. In the central area between Bonito and Porto Murtinho, as well as further south, in Paraguay, slightly foliated homogeneous orthogneisses are widespread. The mineralogy of these rocks is very simple, with quartz, microcline, oligoclase and biotite as main components. This work reports eight U-Pb SHRIMP determinations obtained on zircons. Results are as follows: (1) A basement gneiss yielded a reliable U-Pb zircon age of 1.940 Ma; (2) A monzogranite of the Alumiador Suite yielded a zircon U-Pb age of about 1.830 Ma; (3) Four orthogneisses yielded concordant U-Pb results between 1.700 and 1.760 Ma, suggesting the action of a major tectono-magmatic orogenic event, supported by the available Rb-Sr and Sm-Nd systematics; (4) Very discordant U-Pb zircon ages were obtained on rocks from Paraguay. Their crystals yielded very high uranium contents and were affected by multi-stage Pb loss, that could explain their much younger apparent age compared with the Rb-Sr age on the same rocks. In the area, K-Ar and $^{40}Ar/^{39}Ar$ determinations on micas, with apparent ages close to 1.00 Ma, are indicative of a pervasive regional heating and metamorphism. Taking into account all the available data, the Rio Apa basement rocks seem to correlate well with the Rondonia-Mato Grosso region of the Amazonian Craton, where the Rio Negro-Juruena province is reworked by the Rondonian-San Ignacio Orogeny.

INTRODUCTION

The Rio Apa cratonic fragment, in the central part of South América, is poorly exposed, being covered by extensive Phanerozoic sedimentary sequences. It crops out at the Brazilian border with Bolivia and Paraguay and extends to the south into Paraguayan territory. It is overlain by the Neoproterozoic mainly carbonatic deposits of the Corumbá and Itapocumi Groups, and it is bound to the east by the southern portion of the Paraguay-Araguaia belt of Almeida (1967), folded and regionally metamorphosed during the Brasiliano Orogeny. In this work, a few U-Pb SHRIMP zircon determinations on different rocks from this unit are presented. They are considered together with other geochronological data already available, allowing an improved integrated interpretation of the tectonic evolution of the Rio Apa cratonic fragment. The correlation of this tectonic unit with the much larger Amazonian Craton, and their relative positions in the Proterozoic, is important for the reconstruction of the Rodinia and Gondwana supercontinents (for instance, see Cordani *et al*., 2003).

GEOLOGICAL SETTING

Fig. 1 brings a reconnaissance map of the main area of exposure of the Rio Apa Craton, and its eastern border with the Paraguay-Araguaia belt, in SW Mato Grosso do Sul and northeastern Paraguay. It was made after a re-examination of the previous geological maps produced by Araujo *et al*. (1982); Wiens, (1986); and Godoi *et al*. (1999), plus the observations of the senior author, made during a short trip to the area in 2003, when the samples used in this study were collected.

In the western part of the basement area, a medium-grade metamorphic belt is recognized, made up by gneisses and schists, described as the Rio Apa Complex and the Alto Tererê association of Godoi *et al.* (1999). They are intruded by different types of foliated granitoid rocks. To the south, near Porto Murtinho, these basement rocks are covered by the felsic volcanics of the Amoguijá Group, and are also intruded by the granitoid rocks of the Alumiador Suite of Araujo *et al*. (1982). To these authors, the acid volcanics are considered to be the extrusive equivalents of the Alumiador granites.

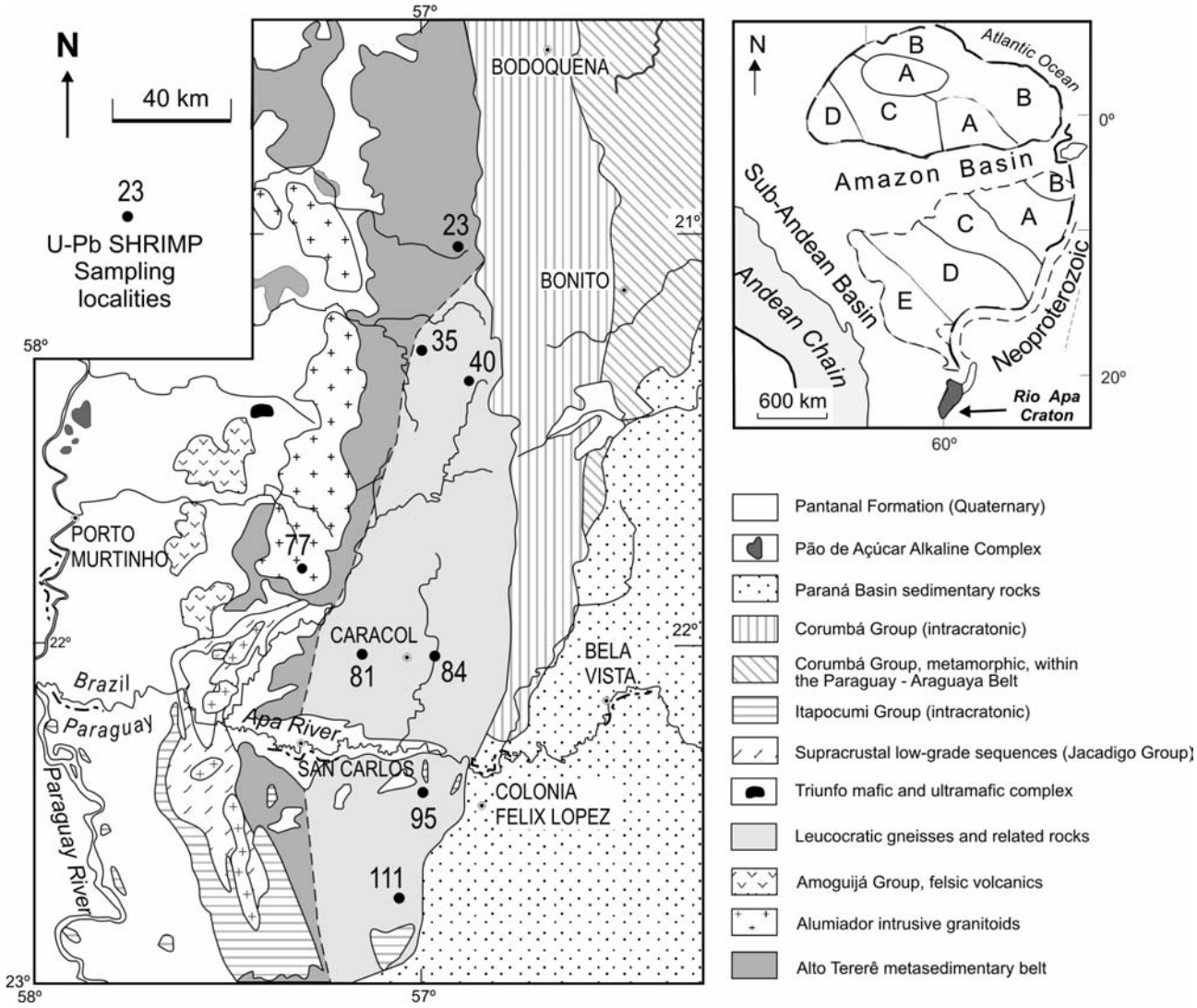

Figure 1. Geological sketch map of the southern part of the Rio Apa cratonic fragment. In the upper diagram, the tectonic provinces of the Amazonian Craton are displayed: A: Central Amazonian Province; B: Maroni-Itacaiunas Province; C: Ventuari-Tapajós Province; D: Rio Negro-Juruena Province and E: Rondonian-San Ignacio and Sunsás provinces.

In the central part of the region, from about the latitude of the town of Bonito, and extending to the south to include the towns of Caracol in Brazil and San Carlos in Paraguay, slightly foliated homogeneous orthogneisses are widespread, and are intruded in many places by isotropic slightly deformed granitic bodies, especially in Paraguay (Wins, 1986). The mineralogy of all of these granitoid rocks is very simple, with quartz, microcline, oligoclase and biotite as main components.

Moreover, supracrustal low-grade metamorphic sequences are identified along the Apa river, at the Brazil-Paraguay border. They are included by Godoi *et al*. (1999) within the Jacadigo Group. Along the Serra de Bodoquena in Brazil, and at the southernmost part of the area, in Paraguay, the intracratonic covers of the Corumbá Group (in Brazil) and Itapocumi Group (in Paraguay) are reported, in which carbonatic sediments predominate. Finally, at the easternmost part of the region, the low-grade metasedimentary rocks of the Paraguay-Araguaia belt occur, exhibiting a clear tectonic and metamorphic polarity related to the imprint of the Brasiliano Orogeny, in the Neoproterozoic.

PREVIOUS RADIOMETRIC RESULTS

Several Rb-Sr and K-Ar geochronological data were obtained for the Brazilian portion of the area by Araujo *et al*. (1982). Additional age determinations, by the Rb-Sr method, as well new data by the Sm-Nd and Ar-Ar methods, were obtained in several granitoid rocks of the basement, some of them in Paraguay, by Cordani *et al*. (2005).

About 40 Rb-Sr whole-rock analyses are now available. Most of them were performed in granitoid rocks, either in the orthogneisses, or in the intrusive Alumiador granitoids. Because they were collected in different outcrops, they cannot be considered strictly cogenetic. However, with a few exceptions, all the analytical points are remarkably aligned in a Rb/Sr isochron diagram, and the calculated best-fit line exhibits a slope corresponding to about 1.700 Ma, with a $^{87}Sr/^{86}Sr$ initial ratio of about 0,706 (Cordani *et al*, 2005). Many samples exhibit high Rb/Sr ratios and apparent Rb-Sr ages can be calculated. A granitic sample in Paraguay yielded the oldest value of 1.840 Ma, while the youngest apparent ages, near 1.440 Ma, were obtained in two granophyres associated to Alumiador granites.

Six Sm-Nd whole-rock determinations were made by Cordani *et al* (2005), and yielded Sm-Nd T_{DM} model ages between 2.200 and 2.530 Ma, as well as slightly negative $\varepsilon_{Nd(1700)}$ values. Sixteen $^{40}Ar/^{39}Ar$ determinations were also obtained for different rocks within the region, and the most significant result is a tight grouping of very precise plateau ages close to 1.300 Ma, shown by seven biotites and five muscovites.

These already available radiometric data are very significant for the timing of relevant episodes in the context of the regional tectonic evolution, and therefore they bring about important constraints for the interpretation of the new U-Pb SHRIMP zircon ages. More specifically, this is the case of the Rb-Sr general reference isochron age close to 1.700 Ma of the orthogneisses. This value is very likely related to a Sr isotopic homogenization episode, connected to the medium- to high grade pervasive metamorphism responsible for the granoblastic texture shown by these rocks. Moreover, the $^{40}Ar/^{39}Ar$ apparent ages close to 1.300 Ma must be associated to a strong thermal episode, with temperature of at least 300 ^{o}C, necessary for the complete release of argon from the micas that affected the entire region.

U-Pb SHRIMP DETERMINATIONS

U-Pb dating was carried out on single zircon crystals from eight samples, employing the SHRIMP II instrument of the Chinese Academy of Geological Sciences, operated from São Paulo using the SHRIMP Remote Operational System (SROS) device. Details of the analytical procedures are presented by Williams (1998). Correction for common Pb was made based on the measured ^{204}Pb, and the typical error component for the $^{206}Pb/^{238}U$ ratios is less than 2 %. Uranium abundance and U/Pb ratios were calibrated against the TEM standard. The analytical results are displayed in Table 1, and the apparent ages are shown in the Concordia diagrams of figures 2A to 2H, drawn at the same scale to allow direct comparison.

Sample 23 from the western basement area is a strongly foliated medium-grade biotite-hornblende gneiss, in which plagioclase (45 %) predominates over microcline (15 %). It also includes quartz (25 %), biotite (10 %) and hornblende (5 %), plus sphene, apatite and epidote. Zircons are mainly subhedral prismatic crystals, 200-300 μm long, with dark oscillatory-zoned cores and small white low-U rims in the CL images. Table 1 indicates U content of 200-500 ppm, as well as quite low common Pb correction In figure 2A, the three most concordant zircons yielded 1.935 ± 15 Ma. The other discordant zircons are disposed along a poorly defined discordia, but tending to an apparent Neoproterozoic episode of Pb-loss.

Samples 35, 40, 81, 84, 95 and 111 are slightly foliated medium to high grade leucocratic orthogneisses, light grey to pink, with very similar mineral composition and textures. They comprise plagioclase (20 to 50 %), microcline (30 to 40 %), quartz (20 to 40 %) and some biotite (usually less than 5 %). Zircon, allanite, apatite, chlorite, epidote and opaques are the common accessories. These rocks exhibit medium grain size, millimetric, and textures are always granoblastic.

Sample 35 includes many euhedral crystals, usually short prismas with pyramid terminations, 50-150 μm long, together with a smaller population of larger crystals, up to 300 μm long. In the CL images oscillatory-zoned cores and relatively large dark overgrowths of high-U zircon are observed. U content is between 250-550 ppm (Table 1), but some zircons show high content, up to 2000 ppm. In figure 2B two nearly concordant zircons yielded an age close to 1.730 Ma, and the other discordant zircons seem to indicate a multi-branched pattern of Pb-loss.

Name	%$^{206}Pb_c$	U ppm	Th ppm	$^{232}Th/^{238}U$ ppm	$^{206}Pb_{Rad}$ ppm	% Di	$^{206}Pb/^{238}U$ Age Ma ± 1sError	$^{207}Pb/^{206}Pb$ Age Ma ±1sError	$^{207}Pb/^{206}Pb$ ± %Error	$^{207}Pb/^{235}U$ ±%Error	$^{206}Pb/^{238}U$ ± %Error
23.1	0.42	248	214	0.89	76.2	-1	1962.5±25.0	1936±22	0.1186±1.2	5.82±1.9	0.3559±1.5
23.3	0.11	459	315	0.71	129.4	5	1828.8±22.6	1920±15	0.1176±0.9	5.32±1.7	0.3280±1.4
23.5	0.09	383	350	0.94	96.3	14	1654.3±20.5	1932±16	0.1184±0.9	4.78±1.7	0.2926±1.4
23.6	0.11	197	165	0.87	59.7	1	1949.7±25.9	1968±19	0.1208±1.1	5.88±1.9	0.3532±1.5
23.7	0.00	228	148	0.67	68.0	2	1919.7±24.9	1955±17	0.1199±1.0	5.73±1.8	0.3469±1.5
23.8	0.55	359	205	0.59	88.0	15	1609.9±20.3	1895±22	0.1160±1.2	4.54±1.9	0.2837±1.4
35-01	0.32	254	257	1.05	64.7	4	1671.4±21.6	1743±27	0.1067±1.4	4.35±2.1	0.2960±1.5
35-02	2.38	446	345	0.80	82.7	18	1232.4±21.1	1499±150	0.0936±7.9	2.72±8.1	0.2107±1.9
35-03	0.87	331	453	1.41	77.9	6	1548.9±19.9	1639±35	0.1008±1.9	3.78±2.4	0.2716±1.4
35-04	0.54	263	282	1.11	62.6	10	1568.9±20.6	1744±30	0.1067±1.6	4.05±2.2	0.2755±1.5
35-05	0.50	553	264	0.49	102.9	18	1258.9±16.2	1531±27	0.0951±1.4	2.83±2.0	0.2157±1.4
35-06	16.61	2048	1197	0.60	140.8	66	416.5±6.9	1242±240	0.0818±12.3	0.75±12.4	0.0667±1.7
35-07	3.55	357	584	1.69	58.4	35	1086.4±18.0	1662±72	0.1021±3.9	2.58±4.3	0.1836±1.8
35-09	0.42	246	206	0.86	62.8	3	1672.9±22.3	1727±29	0.1057±1.6	4.32±2.2	0.2963±1.5
40-1.1	0.62	133	84	0.65	26.4	15	1329.4±35.4	1566±71	0.0969±3.8	3.06±4.8	0.2290±3.0
40-2.1	0.96	319	229	0.74	54.7	32	1162.4±28.4	1710±43	0.1048±2.3	2.85±3.6	0.1976±2.7
40-3.1	0.00	117	105	0.93	31.2	0	1739.6±43.9	1734±35	0.1062±1.9	4.53±3.4	0.3098±2.9
40-4.1	0.24	210	109	0.54	54.4	4	1698.1±40.4	1765±30	0.1079±1.7	4.49±3.2	0.3014±2.7
40-5.1	2.11	137	126	0.94	22.2	28	1089.9±28.8	1519±106	0.0946±5.6	2.40±6.3	0.1842±2.9
40-6.1	2.15	302	238	0.82	73.7	12	1582.0±37.1	1796±50	0.1098±2.8	4.21±3.8	0.2781±2.6
40-7.1	0.16	264	223	0.87	57.9	16	1464.2±34.8	1734±25	0.1062±1.4	3.73±3.0	0.2550±2.7
40-8.1	2.00	254	141	0.57	37.9	42	1012.3±25.6	1734±74	0.1061±4.1	2.49±4.9	0.1700±2.7
40-9.1	0.91	138	137	1.02	30.0	11	1438.3±36.3	1610±63	0.0992±3.4	3.42±4.4	0.2500±2.8
40-10.1	1.42	146	148	1.04	24.5	30	1134.0±29.5	1617±83	0.0996±4.5	2.64±5.3	0.1923±2.8
77-1.1	0.23	190	147	0.80	52.2	5	1783.9±42.2	1879±27	0.1150±1.5	5.05±3.1	0.3188±2.7
77-2.1	14.67	132	114	0.89	39.5	8	1673.3±48.1	1813±247	0.1108±13.6	4.53±14.0	0.2964±3.3
77-3.1	0.13	77	84	1.12	19.1	14	1626.3±43.2	1889±40	0.1156±2.2	4.57±3.7	0.2870±3.0
77-4.1	1.60	666	700	1.09	154.1	15	1515.9±34.9	1787±34	0.1092±1.9	3.99±3.2	0.2651±2.6
77-5.1	1.16	156	168	1.11	44.2	-1	1816.4±45.4	1796±60	0.1098±3.3	4.93±4.4	0.3255±2.9
77-6.1	2.02	266	503	1.95	68.7	7	1664.6±39.0	1787±61	0.1093±3.4	4.44±4.3	0.2946±2.7
77-4.1	1.60	666	700	1.09	154.1	15	1515.9±34.9	1787±34	0.1092±1.9	3.99±3.2	0.2651±2.6
77-5.1	1.16	156	168	1.11	44.2	-1	1816.4±45.4	1796±60	0.1098±3.3	4.93±4.4	0.3255±2.9
77-6.1	2.02	266	503	1.95	68.7	7	1664.6±39.0	1787±61	0.1093±3.4	4.44±4.3	0.2946±2.7
77-7.1	0.15	773	680	0.91	207.2	4	1748.6±38.9	1820±13	0.1112±0.7	4.78±2.6	0.3116±2.5
77-8.1	1.35	133	124	0.96	36.5	5	1763.7±43.5	1854±55	0.1134±3.0	4.92±4.1	0.3147±2.8
77-9.1	5.28	98	82	0.87	15.2	44	1019.6±30.1	1806±172	0.1104±9.4	2.61±10.0	0.1714±3.2
8L-1.1	3.47	2071	2408	1.20	167.9	59	562.0±13.7	1378±57	0.0878±3.0	1.10±3.9	0.0911±2.5
8L-2.1	0.08	297	283	0.98	72.1	9	1600.9±36.7	1768±20	0.1081±1.1	4.20±2.8	0.2819±2.6
8L-4.1	0.40	503	1151	2.37	88.0	28	1190.7±27.8	1649±23	0.1013±1.3	2.83±2.9	0.2029±2.6
8L-5.1	0.46	523	616	1.22	63.3	47	846.3±20.4	1598±29	0.0986±1.5	1.91±3.0	0.1403±2.6
8L-6.1	0.15	664	206	0.32	50.7	-2	548.1±13.5	539±44	0.0582±2.0	0.71±3.2	0.0887±2.6

Name	$\%^{206}Pb_c$	U ppm	Th ppm	$^{232}Th/^{238}U$ ppm	$^{206}Pb_{Rad}$ ppm	% Di	$^{206}Pb/^{238}U$ Age Ma ± 1sError	$^{207}Pb/^{206}Pb$ Age Ma ±1sError	$^{207}Pb/^{206}Pb$ ± %Error	$^{207}Pb/^{235}U$ ±%Error	$^{206}Pb/^{238}U$ ± %Error
8L-7.1	1.24	887	1467	1.71	73.3	61	585.4±14.4	1512±41	0.0942±2.2	1.23±3.4	0.0951±2.6
8L-7.2	0.06	388	379	1.01	82.1	19	1419.8±32.9	1752±19	0.1072±1.1	3.64±2.8	0.2464±2.6
8L-8.1	3.99	679	1431	2.18	49.1	65	500.9±12.7	1450±93	0.0911±4.9	1.02±5.5	0.0808±2.6
8L-9.1	1.00	151	165	1.13	34.5	8	1508.0±37.7	1640±63	0.1008±3.4	3.66±4.4	0.2636±2.8
8L-10.1	0.79	824	1380	1.73	79.2	53	678.7±16.5	1451±34	0.0912±1.8	1.40±3.1	0.1110±2.6
8L-11.1	0.10	239	240	1.04	58.7	9	1620.0±44.5	1773±25	0.1084±1.4	4.27±3.4	0.2857±3.1
84-1	0.20	121	85	0.72	31.9	0	1721.8±25.8	1724±29	0.1056±1.6	4.46±2.3	0.3062±1.7
84-2	0.40	106	90	0.88	29.7	-6	1811.0±27.8	1713±34	0.1049±1.8	4.69±2.6	0.3244±1.8
84-3	0.73	101	75	0.77	27.0	-2	1741.2±27.3	1714±49	0.1050±2.7	4.49±3.2	0.3101±1.8
84-4	0.26	119	95	0.83	32.9	-2	1794.1±26.9	1757±37	0.1075±2.0	4.75±2.6	0.3209±1.7
84-5	0.46	198	237	1.24	52.7	-4	1734.4±23.0	1667±29	0.1024±1.6	4.36±2.2	0.3087±1.5
84-6.1	0.12	151	144	0.98	40.6	0	1751.1±24.8	1757±27	0.1075±1.5	4.63±2.2	0.3121±1.6
84-6.2	0.87	92	71	0.80	24.8	-2	1748.5±27.6	1709±58	0.1047±3.1	4.50±3.6	0.3116±1.8
95-1.1	3.20	2298	144	0.06	246.5	30	735.5±17.6	1050±64	0.0743±3.2	1.24±4.1	0.1209±2.5
95-1.2	1.33	2269	231	0.11	251.7	44	773.1±18.6	1371±42	0.0875±2.2	1.54±3.4	0.1274±2.6
95-2.1	0.49	2337	1099	0.49	355.5	31	1046.3±24.3	1512±16	0.0942±0.8	2.29±2.6	0.1762±2.5
95-3.1	6.37	2250	5227	2.40	149.3	68	449.9±11.3	1426±96	0.0900±5.0	0.90±5.7	0.0723±2.6
95-3.2	1.92	1209	1264	1.08	150.7	44	857.8±20.6	1535±48	0.0954±2.5	1.87±3.6	0.1423±2.6
95-4.1	4.52	1117	756	0.70	145.9	38	873.8±21.0	1410±73	0.0893±3.8	1.79±4.6	0.1452±2.6
95-5.1	1.61	311	128	0.42	51.4	20	1115.6±27.1	1397±61	0.0887±3.2	2.31±4.1	0.1889±2.6
95-5.2	14.11	1427	1529	1.11	198.9	43	841.4±21.4	1472±177	0.0922±9.3	1.77±9.7	0.1394±2.7
95-6.1	1.85	219	17	0.08	38.3	11	1177.2±29.6	1323±102	0.0853±5.3	2.36±6.0	0.2004±2.8
95-7.1	0.49	195	28	0.15	32.5	20	1137.9±29.4	1418±50	0.0897±2.6	2.39±3.9	0.1931±2.8
95-8.1	0.56	420	74	0.18	73.0	13	1182.5±28.2	1355±41	0.0867±2.1	2.41±3.4	0.2013±2.6
95-8.3	6.81	1418	821	0.60	148.5	42	693.7±17.1	1204±118	0.0803±6.0	1.26±6.5	0.1136±2.6
95-9.1	0.17	2224	246	0.11	430.3	21	1307.3±29.8	1647±13	0.1012±0.7	3.14±2.6	0.2248±2.5
111-2.1	5.21	1845	645	0.36	270.7	32	967.1±22.7	1419±68	0.0897±3.6	2.00±4.4	0.1619±2.5
111-2.1	5.21	1845	645	0.36	270.7	32	967.1±22.7	1419±68	0.0897±3.6	2.00±4.4	0.1619±2.5
111-3.1	1.04	1859	298	0.17	268.5	35	992.1±23.1	1525±22	0.0948±1.1	2.18±2.8	0.1664±2.5
111-4.1	0.30	1492	253	0.18	286.0	16	1294.5±29.6	1544±16	0.0958±0.8	2.94±2.7	0.2224±2.5
111-5.1	0.94	905	235	0.27	173.5	24	1287.2±29.5	1690±23	0.1036±1.2	3.16±2.8	0.2210±2.5
111-6.1	0.59	1222	337	0.29	211.1	28	1175.2±27.0	1639±19	0.1008±1.0	2.78±2.7	0.2000±2.5
111-7.1	10.88	2378	1018	0.44	218.5	61	586.9±14.6	1491±127	0.0931±6.7	1.22±7.2	0.0953±2.6
111-8.1	1.72	2107	1009	0.50	233.4	47	769.3±18.2	1462±31	0.0917±1.6	1.60±3.0	0.1268±2.5
111-9.1	0.54	2760	1057	0.40	407.1	20	1016.5±23.5	1275±14	0.0832±0.7	1.96±2.6	0.1708±2.5
111-10.1	4.37	1619	667	0.43	251.0	34	1026.6±24.0	1559±55	0.0966±2.9	2.30±3.9	0.1726±2.5
111-11.1	7.14	1363	617	0.47	216.2	33	1020.3±24.7	1516±106	0.0944±5.6	2.23±6.2	0.1715±2.6

Table 1: Analytical data of the U-Pb SHRIMP age determinations.

In sample 40, zircons are mainly large subhedral crystals, with pyramidal terminations, 200-300 μm long. They are dark brown, and heavy fractured. The CL images are complex, showing oscillatory-zones but also

some sector-zoned cores, together with many oscillatory-zoned overgrowths. Small dark rims are observed, as well as embayments filled with high-U zircon. Table 1 shows moderate U content of 110-320 ppm, and usually low common Pb correction. In figure 2C, two concordant zircons indicate an age of 1.752 ± 46 Ma, and many other discordant zircons exhibit large scattering along split discordias generated by effects of multi-stage Pb-loss. In general, they seem to bear a tendency to a Neoproterozoic lower intercept.

Sample 81 includes a population of subhedral to euhedral prismatic zircons, 80-200 μm long, some rounded and exhibiting resorption features. CL images show complex structures, with cores of different types as well as borders and embayments with high-U filling. U content is very variable, usually between 150-900 ppm. One zircon crystal had more than 2000 ppm. Figure 2D shows that the two most concordant point's yielded $^{207}Pb/^{206}Pb$ ages of about 1.750 Ma. Many discordant zircons were scattered along different discordias resulting from multi-stage Pb-loss. In addition, one concordant crystal showed a much younger age, of 540 Ma, suggesting the possibility of some growth of new zircon during the Neoproterozoic.

Sample 84 presents subhedral to anhedral short prismas, 80-150 μm long. The CL images show light grey cores with igneous zoning and white low-U rims. Table 1 indicates U content between 100 and 200 ppm, and usually low common Pb corrections. Figure 2E shows that practically all measured crystals are concordant or slightly discordant, with an average age of 1.721 ± 26 Ma.

Sample 95 presents large fragments of anhedral crystals, 150-350 μm long, many of them rounded and with evidence of resorption. The CL images show complex structures, in which cores are in part sector-zoned metamorphic-type, and in part made up by magmatic oscillatory-zoned zircon. The crystals have dark borders and many embayments and fractures filled with high-U zircon. Table 1 shows U contents usually high, some grains with 200-420 ppm, some with 1100-1400 ppm, and several with more than 2200 ppm. Most cases show large common Pb correction. Figure 2F shows that all crystals are discordant, scattered along split discordias dominated by recent Pb-loss. Many crystals are relatively close to Concordia at 1100-1.200 Ma.

Sample 111 presents anhedral crystals and fragments, mainly 100-220 μm long, very similar to those of sample 95. Most of them are completely dark with CL-luminescence embayments, indicating resorption and metamorphic replacement. U content of the crystals is usually very large, with at least 900 ppm, and some grains with up to 2.800 ppm. In figure 2G, all grains are discordant, showing multi-stage Pb diffusion, dominated by recent Pb-loss.

Sample 77 is a pink unfoliated monzogranite of the Alumiador Suite. Its mineral composition includes plagioclase, microcline and quartz in similar amounts, around 30 %, plus biotite (less than 10 %), sphene, zircon, epidote, apatite and opaques. Texture is equigranular, magmatic-type, with millimetric grain size, but including some centimeter-size K-feldspar crystals. In this sample, large euhedral to subhedral prismatic zircon crystals, 180-300 μm long, are found. CL images show oscillatory-zoned cores and dark (possibly magmatic) resorbed borders. The crystals are dark brown, fractured, and showing filling with high-U zircon. Table 1 shows that U content is variable, usually within 70-270 ppm, but with some high-U crystals, up to 800 ppm. In Fig. 2H, four concordant crystals yielded a mean age of 1.829 ± 21 Ma, whilst several discordant zircons are aligned along a poorly defined discordia.

DISCUSSION OF THE U-Pb SHRIMP AGES

In both cases of samples 23 and 77, the few concordant grains makes possible to interpret them in the conventional way, relating their ages to the episodes of magmatic crystallization of their protoliths. Therefore the age of sample 23, 1.935 ± 15 Ma, is the first indication for the existence of a Paleoproterozoic magmatic arc in the basement of the Rio Apa Craton. The age of sample 77, 1.829 ± 21 Ma, represents the intrusive event of the Alumiador Suite. In both cases, a few discordant points indicate the incidence of lead loss, during later events of the tectonic evolution.

Considering the orthogneisses of the central-southern region, only for sample 84 a clear indication is given for the age of its protolith, at 1.721 ± 26 Ma. Good indications are also given by samples 39, 40 and 81, where in each case a small cluster of near concordant analyses is observed, with an age between 1,700 and 1.760 Ma. However, for the two southernmost samples, 95 and 111, the analytical points are extremely discordant, precluding the definition of a reliable upper intercept. In a general way, for all of the six orthogneiss samples, the scatter of the discordant points in the Concordia diagrams does not indicate a unique trend, but a multi-branched pattern of Pb diffusion, achieved by successive Pb-loss episodes.

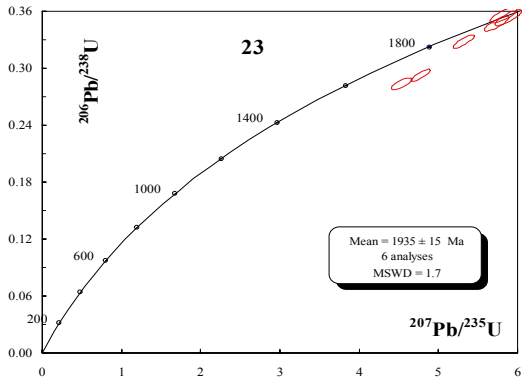

Figure 2A. Sample 23

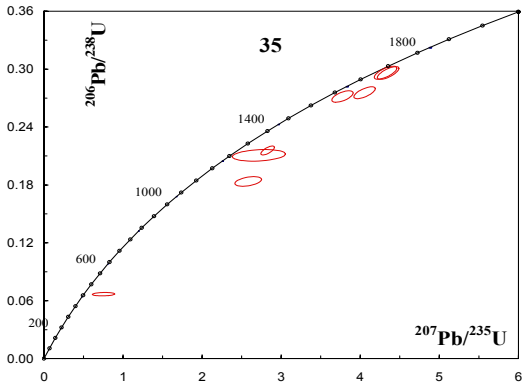

Figure 2B. Sample 35

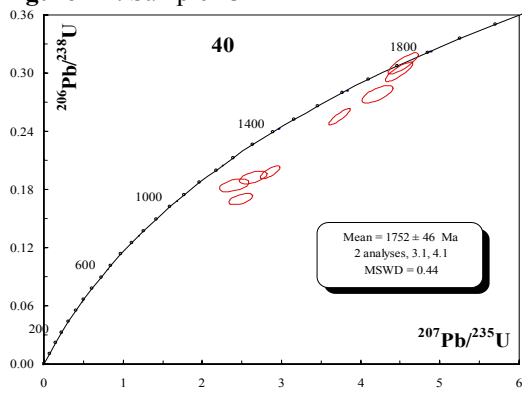

Figure 2C. Sample 40

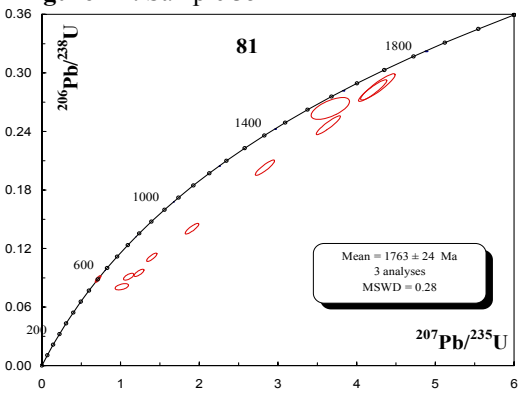

Figure 2D. Sample 81

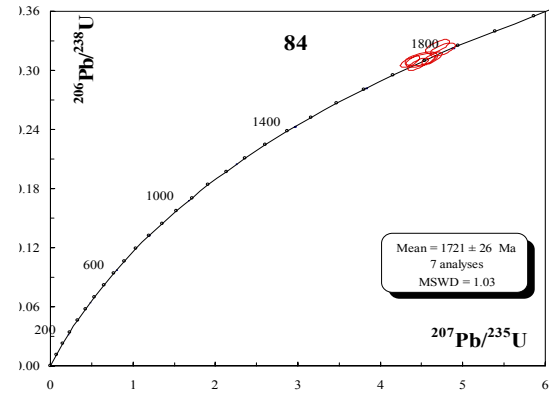

Figure 2E: Sample 84

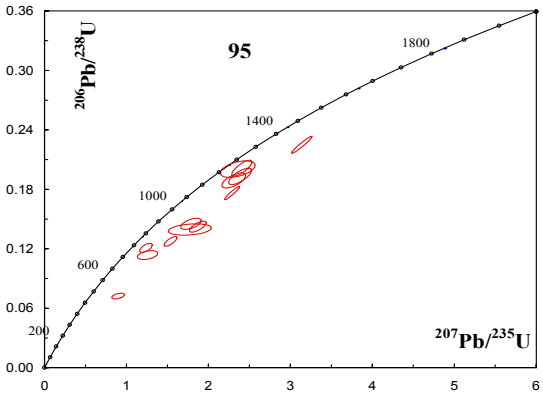

Figure 2F: Sample 95

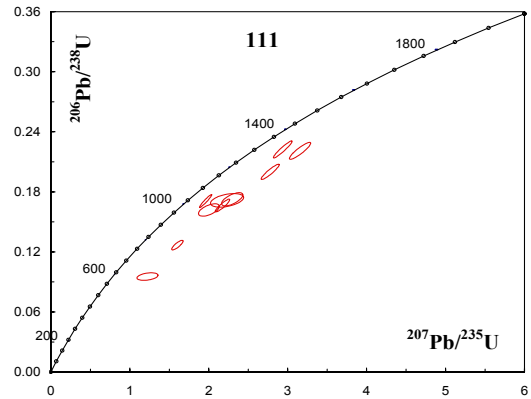

Figure 2G: Sample 111

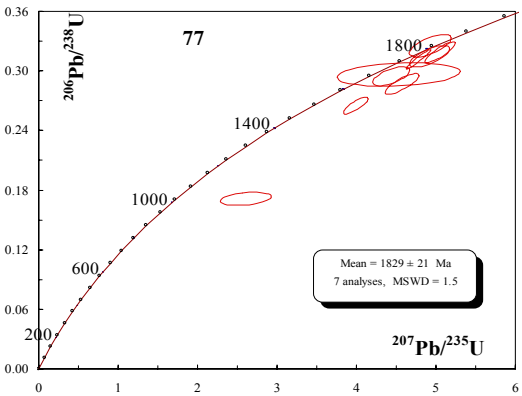

Figure 2H: Sample 77

Figure 2. U-Pb Concordia diagrams for the analysed zircon samples

The number of analyses is not sufficient for a statistical approach; however, looking carefully at all the diagrams, especially those of samples 40, 81, 95 and 111, the scattering about the discordia trends appear to be dominated by recent Pb-loss, as a consequence of alteration over metamict zircon crystals. However, there is also evidence of possible specific Meso and Neoproterozoic Pb-loss episodes related to regional thermal and/or metamorphic episodes.

CONCLUSIONS

Taking into account all the available geochronological data, the tectonic evolution of this part of the Rio Apa cratonic fragment can be envisaged as follows:

1- A basement gneiss yielded a Paleoproterozoic U-Pb zircon age of 1.940 Ma, the first one in this part of the South American continent. This basement is intruded by the Alumiador Suite, of which a monzogranite yielded a reliable age of 1.830 Ma.

2- To the east-southeast of this area, several orthogneisses, formed probably in a series of successive magmatic arcs, between 1.700 and 1.760 Ma, were regionally metamorphosed at medium to high level at about 1.700 Ma, as indicated by Rb-Sr whole-rock work (Araujo *et al*., 1982; Cordani *et al*., 2005).

3- A pervasive regional heating, indicated by several $^{40}Ar/^{39}Ar$ plateau ages on biotites and muscovites (Cordani *et al*., 2005) occurred at about 1.300 Ma, when the temperature for the entire region was higher than 300 ^{o}C.

4- At the eastern border of the area the Paraguay-Araguaia belt was formed (Almeida, 1967), and its tectonic evolution occurred during the latest Neoproterozoic.

Given the tectonic evolution described above, the Rio Apa cratonic fragment correlates well with the Rondonia-Mato Grosso region of the Amazonian Craton, where Mesoproterozoic rocks of the Rio Negro tectonic province, with ages between 1.550 and 1.780 Ma, are reworked by the Rondonian-San Ignacio orogeny, with a strong metamorphic imprint at about 1.300 Ma (Cordani and Teixeira, 2007). This may imply that the Rio Apa cratonic fragment was continuous to the Amazonian Craton, at least in the late Mesoproterozoic, and possibly also in Neoproterozoic times as preconized by Almeida (1967).

REFERENCES:

Almeida, F.F.M.de. 1967. Origem e Evolução da Plataforma Brasileira. Div. Geol. Mineral- DNPM, Rio de Janeiro, Bol 241: 1-36.

Araújo, H.J.T. de, and seven co-authors. 1982. Geologia Folha SF.21, Campo Grande. In: Brasil, Projeto RadamBrasil, Levantamento de Recursos Naturais, 28 Rio de Janeiro, 416 pp.

Cordani U.G. and Teixeira, W. 2007, Proterozoic accretionary belts in the Amazonian Craton. In:Hatcher, R.D.Jr., Carlson, M.P., McBride, J.H. and Martinez-Catalan, J.R. (Eds): 4-D Framework of Continental Crust: Geological Society of America Memoir 200.

Cordani U.G., Tassinari, C.C.G., and Rolim, D.R. 2005 – The basement of the Rio Apa Craton in Mato Grosso do Sul (Brazil) and northern Paraguay: a geochronological correlation with the tectonic provinces of the south-western Amazonian Craton. Gondwana 12, Mendoza (Argentina). Abstracts: 112.

Cordani, U.G., D'Agrella-Filho, M.S., Trindade, R., and Brito-Neves, B.B. 2003. Tearing up Rodinia. Terra Nova. 15: 350-359.

Godoi, H.O, Martins, E.G., and Mello, J.C.R. 1999. CPRM-Programa levantamentos geológicos básicos do Brasil, Folhas Corumbá, Aldeia Tomázia e Porto Murtinho, 65 pp.

Wins. F. 1986. Zur lithostratigraphischen, petrographischen und strukturellen Entwicklung des Rio-Apa Hochlandes, Nordost Paraguay. Clausthal geowiss. Diss. 19: 280 pp